



HAL
open science

Magnetic behaviour of GOES wound cores of transformers fed by square or sine voltages

Daniel Roger, Mathieu Rossi, Houssam Ichou, Jonathan Blaszkowski

► **To cite this version:**

Daniel Roger, Mathieu Rossi, Houssam Ichou, Jonathan Blaszkowski. Magnetic behaviour of GOES wound cores of transformers fed by square or sine voltages. 25th Soft Magnetic Materials Conference (SMM), Sep 2021, Grenoble, France. hal-04306107

HAL Id: hal-04306107

<https://univ-artois.hal.science/hal-04306107>

Submitted on 1 Dec 2023

HAL is a multi-disciplinary open access archive for the deposit and dissemination of scientific research documents, whether they are published or not. The documents may come from teaching and research institutions in France or abroad, or from public or private research centers.

L'archive ouverte pluridisciplinaire **HAL**, est destinée au dépôt et à la diffusion de documents scientifiques de niveau recherche, publiés ou non, émanant des établissements d'enseignement et de recherche français ou étrangers, des laboratoires publics ou privés.

Magnetic behaviour of GOES wound cores of transformers fed by square or sine voltages

Daniel Roger^a, Mathieu Rossi^a, Houssam Ichou^a, Jonathan Blazkowski^b

^aUniv. Artois, UR 4025 - Laboratoire Systèmes Electrotechniques et environnement (LSEE), 62400 Béthune, France

^bthyssenkrupp Electrical Steel, 62330 Isbergues, France.

Abstract – Medium-frequency high-power transformers can be designed with wound magnetic cores made of grain oriented electrical steel (GOES) thin strips. At medium frequencies, eddy currents losses are much higher than for standard applications, the core is hotter than usual. Core losses measurements are made on an experimental testing bench designed for allowing a core much hotter than coils. These measurements show that the global core losses decrease with temperature. With a transformer design inspired from the testing bench, it is possible to reduce the core and the winding volumes for the same medium-frequency transformer rated power with similar efficiencies. Experimental results show also that, for core temperatures up to 250°C, core losses are lower for rectangular voltages than for sine ones at the same peak flux and frequency. Moreover, with rectangular voltages, the power electronic converter structure can be very simple. A detailed Fourier analysis, made for low flux densities, proposes an interpretation of this non-intuitive experimental result and define the limits of the possible pulse widths.

Keywords - Medium frequency transformer; GOES wound core; Global core losses; Eddy current losses; high temperature core.

1. Introduction

With more and more intermittent renewable sources, the electric grid stability is more difficult to achieve [1]. Solid-State Transformers (SSTs) can perform bidirectional real-time power controls in critical nodes of the grid that can improve the global stability [2]. For designing high power SSTs (over 500 kVA) losses in electronic components are a major issue [3, 4]. A solution consists in operating at medium frequencies with power electronic converters that have a basic structure for reducing switching losses [5, 6]. The transformer performances become the main issue of the design of such SSTs [7, 8]. For high-power medium-frequency applications, GOES cores is a good solution [9] because it has a stable crystalline structure that offers long-life spans at a reasonable cost [10].

The paper presents a transformer structure that allows a hot GOES wound core inside coils at a much lower temperature. Core losses are measured for several core temperatures using sine and rectangular voltages. Experimental results show that cores losses are lower for rectangular voltages than for sine waves. They decrease with the core temperatures. This result can be applied to the design of compact efficient and reliable SSTs at a reasonable cost. The paper proposes also an explanation of the lower core losses for rectangular voltages than for sine ones at the same peak flux density and frequency. The well-known diffusion equation of the field inside a sheet of metal is applied using Fourier series for defining a practical limit of the width of rectangular pulses.

2. Experimental approach

A. Mechanical structure

Because of the high permeability of GOES, the wound core presented in Fig. 1 can be made of long strips offering large windows for coils with a reasonable magnetising current. This core is placed in the mechanical structure of Fig. 2 that makes it possible a core hotter than coils. The metallic fixing frame provides also a degree of freedom for the core

thermal expansion. The coil support is fixed directly on the mechanical structure by 8 rods. There is no contact point between the core and the winding, but a 5 mm wide gap. The large temperature difference between the core and the winding is possible with a vertical air flow in this 5mm gap. Two small centrifugal fans (9.6 m³/h at 24 V DC) provide this air flow.



Fig. 1. wound core made with thin GOES strips.

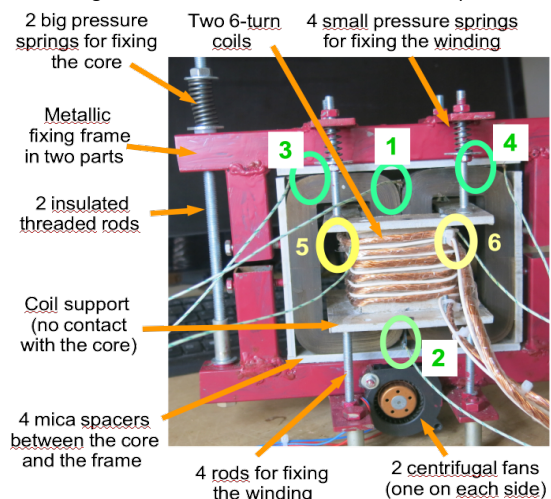


Fig. 2. Medium frequency transformer structure based on a GOES wound core hotter than coils. The metallic fixing frame (in red) avoid any contact between the hot core and the winding.

B. Temperature and core losses measurements

The mechanical structure of figure 2 is used for measuring temperatures and core losses at medium frequencies for sine and rectangular voltages. The winding is made of two 6-turn coils. The primary is made with a Litz wire in order to

limit the additional power created by the magnetizing current. The core losses are computed from the secondary voltage and the primary current for sine and rectangular supplies. Figure 3 presents the testing bench. The bandwidth of the current probe is 240 kHz and 50 MHz for the voltage one; the probe DC offsets are eliminated. The oscilloscope records the signals on 8 periods exactly with 250,000 points. The average flux density is computed by integration of the secondary voltage v_s .

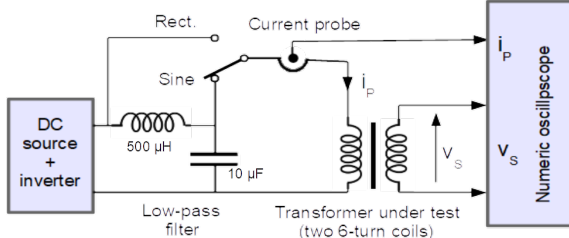


Fig. 3. Testing bench for core losses measurements.

The thermocouples T1-T4 in the green circles of Fig. 2 provide core temperature measurements while T5 and T6 give the winding temperatures. Figure 5 presents an example of transient temperature for 1.2 T peak at 4 kHz and rectangular voltages. For this test, the DC voltage feeding the two centrifugal fans is reduced from 24 V to 18 V for getting core temperatures over 250°C; the actual air flow is reduced to 5.2 m³/h per fan. The coil temperatures (T5, T6) are much lower than the core ones (T1 – T4). The red dotted line is the average core temperature for a rectangular voltage.

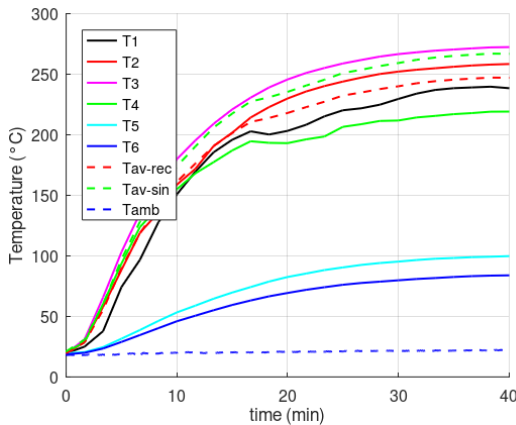


Fig. 5. Transient temperatures at each measurement point and core average temperature T_{av} for rectangular and sine voltages at 4kHz and 1.2 T / 4 KHz.

The core losses are computed from the primary current i_p and the secondary voltage v_s recorded every 2 minutes during the thermal transient. After switching from rectangular voltages to sine ones, the DC source that feeds the inverter is increased for getting an identical peak flux density (1.2 T) and the same experiments are repeated during another thermal transient. The average core temperature is added in Fig. 5 (green dotted line).

Figure 6 presents a synthesis of the 40 recorded files. The 2 core average temperature curves, obtained for rectangular and sine voltages, are used for determining the 2 times that correspond to the same core average temperature. Then, the 2 closest experimental files are used for computing the losses.

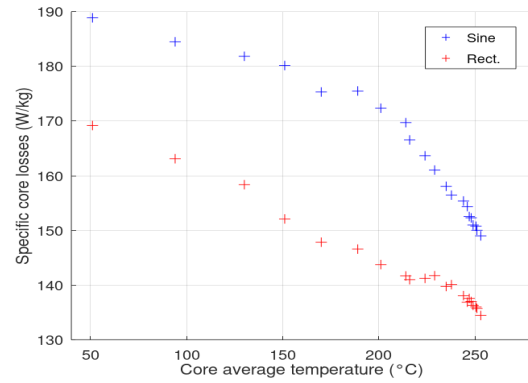


Fig. 6. Specific core losses variations with temperature at 1.2 T – 4 kHz.

This test shows that the global specific core losses decrease with the core temperature. It shows also that the core losses are lower for rectangular voltages than for sine ones. Similar results are observed for every test made in the kHz range, when skin effects in the GOES strip is dominant.

Figure 5 shows that coil temperatures are about 100°C for steady state. Let us now consider an actual transformer made with the same core, the same structure and a winding made with class C (200°C) enamelled wire. The maximum current, defined for the winding maximum temperature, will produce copper losses that will increase all the temperatures of about 100°C. The core losses will be lower while the core temperature remains much under the capabilities of the GOES strips that can operate up to 500°C [11].

3. Interpretation based on Fourier Analysis

The experimental constatation of a reduction of core losses with the temperature increase is easy to understand because of the natural increase of the resistivity of every metal that reduces eddy current losses. The Bertotti formula cannot be applied when the field in the core is not homogenous [12], but the principle of splitting core losses in static, eddy currents and excess losses can help to explain these results. However, the lower core losses for rectangular voltages, that includes harmonics, is more difficult to understand. This phenomenon can be explained using Fourier series: the skin effect is different for each harmonic. The application of Fourier series can only be made in linear conditions, for low flux densities. Maxwell equations are applied to the strip sample of Fig. 7 situated inside the GOES wound core.

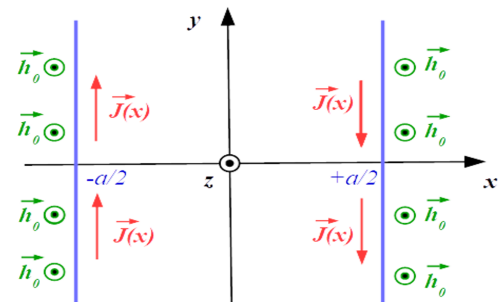


Fig. 7. Strip sample inside the GOES wound core, field between strips. The flux density \vec{B} is in the rolling direction \vec{z} . The strip thickness is noted a and the core width b . The average

length of the core is noted l and the total number of GOES strips N_s .

In a transformer, the primary voltage wave form imposes the time derivative of the flux in the core and, consequently, the average flux density waveform in each GOES strip. The input variable of this electromagnetic problem is this average flux density, not the field \vec{h}_0 at the strip borders.

Figure 8 shows the voltage waveforms (in blue) and the input variables of the electromagnetic problem (in red). The peak average flux density is fixed to 0.4 T in order to be in linear conditions everywhere in the GOES strip sample despite the skin effect. These curves are plotted using Fourier series (1) and (2) limiting the maximum rank to 100. In (1), E is the DC source voltage of the inverter, β angle corresponding to the positive and negative pulse width, n the harmonic rank and ω the angular frequency.

$$\underline{v}_{1n} = \left(E \frac{2}{n\pi} \sin\left(n \frac{\beta}{2}\right) \right) (1 - e^{-jn\pi}) \quad (1)$$

(2) is deduced from (1) by temporal integration adding N_T , the turn number of the primary coil ($N_T = 6$).

$$\underline{\leq B \geq}_n = \frac{\underline{v}_{1n}}{N_T N_s a b} \frac{1}{jn\omega} \quad (2)$$

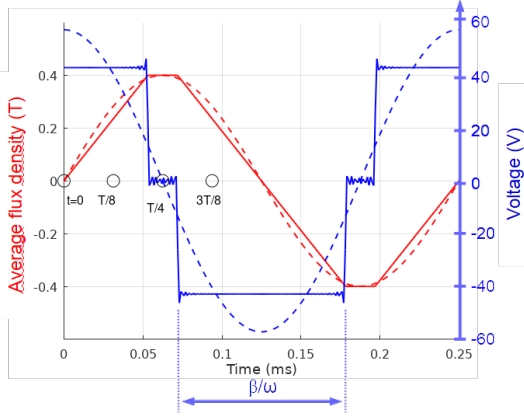


Fig. 8. Average flux densities in the core sample imposed by the primary voltage (solid lines for a rectangular voltage, dotted lines for a sine one). Maxwell equations are solved in 5 steps considering (2) as the problem input.

- The field at any point inside the metal is expressed by the well-known diffusion equation (3), which depends on the field imposed at the strip borders $x = \pm a/2$. However this field is not the input variable, its Fourier series \underline{h}_{0n} , will be determined in a further step. In (3), the complex propagation factors $\underline{\gamma}_n = (1 + j)/\delta_n$ depend on the skin depths $\delta_n = \sqrt{2/(n\omega\mu\sigma)}$. The material permeability μ and its electric conductivity σ are the two other parameters.

$$\underline{h}(x)_n = \underline{h}_{0n} \frac{\cosh(\underline{\gamma}_n x)}{\cosh(\underline{\gamma}_n a/2)} \quad (3)$$

- The average flux density (4) is obtained by a spatial integration of (3) from one border to the other.

$$\underline{\leq B \geq}_n = \frac{1}{a} \int_{-a/2}^{a/2} \mu \underline{h}(x)_n dx = \frac{2 \mu \underline{h}_{0n}}{a \underline{\gamma}_n} \tanh\left(\underline{\gamma}_n \frac{a}{2}\right) \quad (4)$$

- The unknown Fourier series \underline{h}_{0n} is now deduced from the input data (2) using (5).

$$\underline{h}_{0n} = \frac{\underline{\leq B \geq}_n a \underline{\gamma}_n}{2 \mu \tanh\left(\underline{\gamma}_n a/2\right)} \quad (5)$$

- The current densities at any point in the strip $\underline{J}(x)_n$ is obtained by a spatial derivation of (3).

$$\underline{J}(x)_n = -\underline{\gamma}_n \underline{h}_{0n} \frac{\sinh(\underline{\gamma}_n x)}{\cosh(\underline{\gamma}_n a/2)} \quad (6)$$

- For calculating the power densities due to eddy currents, the instantaneous value of the local current density $J(x, t)$ is necessary before calculating its square at any point x for any time t in (8).

$$J(x, t) = \Re\left(\sum_n \underline{J}(x)_n e^{jn\omega t}\right) \quad (7)$$

$$p_v(x, t) = J^2(x, t)/\sigma \quad (8)$$

Figure 9 shows the flux density distribution inside the strip at 4 times emphasised in Fig. 8 for a rectangular voltage (solid lines) and for a sine one (dotted lines). The skin effect is a major phenomenon for both waveforms. The maximum value at the borders is about twice the average peak flux density at $t = T/8$.

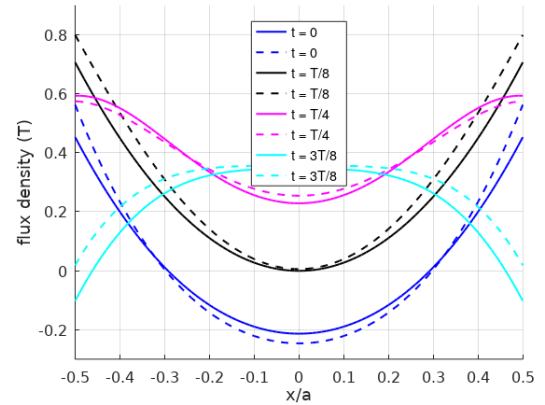


Fig. 9. Flux density at any point inside the GOES strip at $T=0$; $T/8$; $T/4$ and $3T/8$ for a rectangular voltage (solid lines) and for a sine one (dotted lines). These curves are computed with the Fourier series (3) and (5).

Figure 10 shows the power densities inside the strip at the same times with the same graphical conventions. For this pulse width β/ω , most of dotted lines are over the solid lines; the eddy current losses are higher for sine voltages

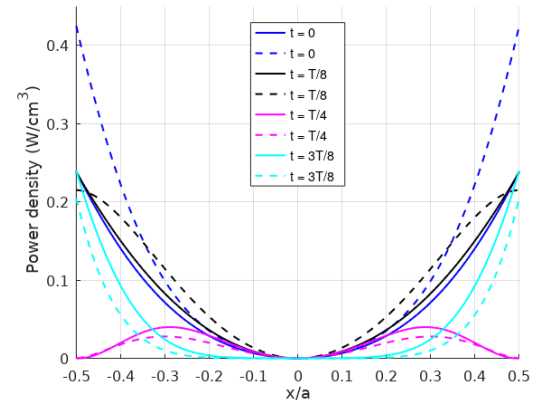


Fig. 10. Power densities due to eddy currents at any point inside the GOES strip at $T=0$; $T/8$; $T/4$ and $3T/8$ for a rectangular voltage (solid lines) and for a sine one (dotted lines).

Figure 11 shows the average value of the eddy current losses computed for several pulse width β/ω at 4 kHz. The pulse voltage is computed for getting the same peak average flux

density (blue line); Eddy current losses are lower for rectangular voltages only for wide voltage pulses ($\beta > 0.77\pi$).

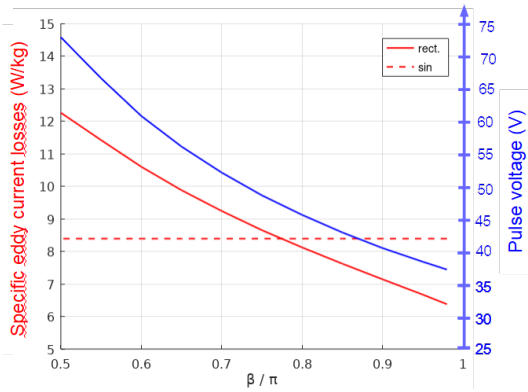


Fig. 11. Specific eddy current losses for several pulse widths and voltages for obtaining 0.4 T peak at 4 kHz.

4. Conclusion

Ampere and Faraday laws applied to a transformer show that the apparent power density is proportional to $B_m \cdot f$ (flux density in the core * frequency). The limits are due to copper and core losses and, consequently, to thermal limits. Copper losses increase with coil temperatures because of the natural increase of copper resistivity. The experimental results of section 2 show that core losses decrease with temperature. Therefore, compact high-power medium-frequency transformers can take the benefits of the high temperature capabilities of GOES wound cores with hot cores inside much colder coils. For a given rated power, higher core temperatures open the way to smaller cores and coils with lower global losses despite the higher core specific losses. The proposed structure shows that this apparent contradiction can be solved by a small air-flux in a free space between the core and the coils.

The Fourier series used for calculating eddy current losses in the GOES wound core at low average flux densities (linear zone of the B(H) curve) helps to explain the measured phenomena. However, its application must be made with two variables (x and t). A too fast interpretation of the harmonic contents can produce erroneous conclusions. For wide voltage pulses, the voltage harmonics do not create additional eddy current losses because they change the current density distribution inside GOES strips.

With the proposed transformer structure, the high-power electronic converters can be made with simple low-cost structures that produce a single pulse per half-period and low switching losses. The global efficiencies of large medium-frequency SSTs designed with this principle are higher than for classical SSTs operating at higher frequencies.

5. References

[1] I. M. Dudurych, "The Impact of Renewables on Operational Security: Operating Power Systems That Have Extremely High Penetrations of Nonsynchronous Renewable Sources," in *IEEE Power and Energy Magazine*, vol. 19, no. 2, pp. 37-45, March-April 2021.

[2] J. Ostergaard, C. Ziras, H. W. Bindner, J. Kazempour, M. Marinelli, P. Markussen, S. H. Rosted, and J.S. Christensen, "Energy Security

Through Demand-Side Flexibility: The Case of Denmark," *IEEE Power and Energy Magazine*, 2021, 19, 46-55.

[3] M. A. Bahmani, T. Thiringer and M. Kharezy, "Design Methodology and Optimization of a Medium-Frequency Transformer for High-Power DC-DC Applications," in *IEEE Transactions on Industry Applications*, vol. 52, no. 5, Sept.-Oct. 2016, pp. 4225-4233.

[4] M. Rylko, K. Hartnett, J. Hayes and M. Egan, "Magnetic material selection for high power high frequency inductors in dc-dc converters," in *Applied Power Electronics Conference and Exposition*, Feb. 2009, pp. 2043-2049.

[5] P. Huang *et al.*, "Optimal Design and Implementation of High-Voltage High-Power Silicon Steel Core Medium-Frequency Transformer," in *IEEE Transactions on Industrial Electronics*, vol. 64, no. 6, pp. 4391-4401, June 2017, doi: 10.1109/TIE.2017.2674591.

[6] H. Ichou, D. Roger, M. Rossi, T. Belgrand, R. Lemaitre, "Assessment of a grain oriented wound core transformer for solid state converter," *Journal of Magnetism and Magnetic Materials - JMMM* 504, March 2020.

[7] S. E. Zirka, Y. I. Moroz, Ph. Marketos, A. J. Moses, "Evolution of the loss components in ferromagnetic laminations with induction level and frequency," *Journal of Magnetism and Magnetic Materials* 320 (2008) e1039-e1043.

[8] B. S. Ram, A. K. Paul, S.V. Kulkarni, "Soft magnetic materials and their applications in transformers," *Journal of Magnetism and Magnetic Materials* 537 (2021) 168210.

[9] T. Kaudera, T. Belgrand, R. Lemaitre, A. Thula, K. Hameyer, "Medium-frequency power transformer using GOES for a three-phase dual active bridge," *Journal of Magnetism and Magnetic Materials* 504 (2020) 166672.

[10] R. Lemaitre, T. Belgrand, "Matériaux magnétiques doux cristallins. Acier électrique á grains orientés," *Techniques de l'ingénieur* (2014).

[11] M. Ababsa, O. Ninet, G. Velu, J. Lecoite, "High temperature magnetic characterization using an adapted Epstein frame," *IEEE Trans. Magn.* 54 (6) (2018) 1-6.

[12] G. Bertotti, "General properties of power losses in soft ferromagnetic materials," *IEEE Transactions on Magnetics*, vol. 24, no. 1, Jan. 1988, pp. 621-630.